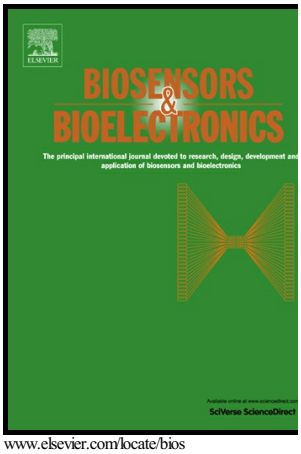

Sensitive and rapid detection of pathogenic bacteria in small volumes using impedance spectroscopy technique

Namrata Pal, Shashank Sharma, Shalini Gupta

www.elsevier.com/locate/bios

PII: S0956-5663(15)30433-4
DOI: http://dx.doi.org/10.1016/j.bios.2015.09.037
Reference: BIOS8004

To appear in: *Biosensors and Bioelectronic*

Received date: 18 May 2015
Revised date: 13 September 2015
Accepted date: 15 September 2015

Cite this article as: Namrata Pal, Shashank Sharma and Shalini Gupta, Sensitiv and rapid detection of pathogenic bacteria in small volumes using impedanc spectroscopy technique, *Biosensors and Bioelectronic* http://dx.doi.org/10.1016/j.bios.2015.09.037

Sensitive and Rapid Detection of Pathogenic Bacteria in Small Volumes using Impedance Spectroscopy Technique

Namrata Pal, Shashank Sharma[#] and Shalini Gupta[*]

Department of Chemical Engineering, Indian Institute of Technology Delhi, Hauz Khas, New Delhi, India 110016

*Corresponding author. E-mail: shalinig@chemical.iitd.ac.in

Graphical abstract

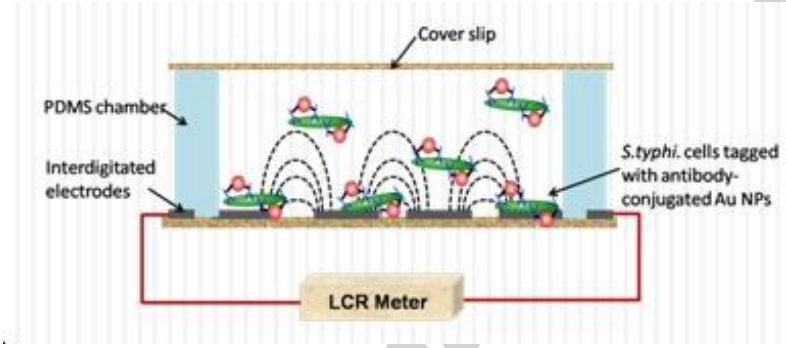

Abstract

We illustrate a novel impedance immunosensor which rapidly and sensitively detects typhoid-causing infectious bacteria Salmonella enterica serovar (S. typhi) in 10 μL of sample volume. The bacteria are tagged with gold nanoparticles (Au NPs) via high-affinity antigen-antibody interactions for enhanced signal amplification and selectivity. The cell-particle bioconjugates are then subjected to alternating current (AC) electric fields applied through interdigitated microelectrodes. The immunosensor performance is optimized with respect to electric field frequency, cell concentration, incubation times and the type of blocking agent to achieve a low limit of detection (LOD) of 100 CFU/mL. The approach is extendable to a wide spectrum of clinical diseases and offers an efficient and cost-effective solution for point-of-care diagnosis.

Keywords: Impedance, gold nanoparticle, detection, Salmonella, biosensor, typhoid

1. Introduction

Infectious diseases caused by pathogenic bacteria or viruses are notoriously difficult to diagnose as the concentration of the causative agents is low especially in the initial phase of illness. In the case of enteric fever (commonly known as typhoid), the concentration of S. typhi bacteria in blood never exceeds beyond 1 to 10 CFU/mL during the entire course of illness making it a rare cell disease like metastatic cancer (Wain et al., 1998; Zhou et al., 2008). Identification of such low bacterial concentrations particularly in the presence of large background cell blood components like erythrocytes (~ 10^9 cells/mL) and leukocytes (~ 10^6 cells/mL) is a mammoth task that poses a great challenge in early detection of blood-borne infectious diseases. The two current mainstream diagnostic methodologies for in vitro detection are cell culture growth followed by biochemical testing and the more labor intensive polymerase chain reaction (PCR) technique, both of which are highly time consuming and easily prone to false negative results (Garibyan and Avashia, 2013; Ahmed et al., 2014; Yang and Bashir, 2008; Ye, R., 2010).

To overcome the present limitations, researchers over the past two decades have strived to develop affordable and miniaturized biosensing devices that can perform a host of complex bioanalytical processes on a single chip such as immunoassays, DNA analysis, whole cell separation and detection, sample enrichment, tissue engineering or drug discovery (Gervais et al., 2011; Khandurina et al., 2000; Sanders and Manz, 2000; Tsai et al., 2015; Yoon and Kim, 2012). The advent of these new technologies has revolutionized the medical research field as the microdevices require significantly less sample volumes and power consumption. They also enable higher throughput, enhance sensitivity and specificity of signal, minimize user intervention and lower the cost of analysis per test (Yadav et al., 2009; Yeo et al., 2011). The only technical challenge that remains to be addressed is the true point-of-care nature of these

devices. Many microfluidic lab-on-chip systems for instance, use optical microscopy, light scattering, surface plasmon resonance spectroscopy or other such equivalent techniques for quantifying biomolecular binding events (Ko and Grant, 2006; Wen et al., 2013). While these approaches are highly sensitive, they are not the best way forward in terms of cost and simplicity of miniaturization since most optical detection systems require bulky components, and tend to be low throughout due to the small cross-sectional area of the focus beam available for data collection.

Electrical detection through surface patterned electrodes, in this regard, is a more facile and scalable technique for early disease diagnosis since the signal generation can be readily multiplexed, automated and interfaced with other digital devices. The signals can also be measured in real-time with high sensitivity over miniaturized surface areas enabling portability (Melvin et al., 2011; Yang, L., 2008; Yang et al., 2004; Zhu et al., 2010). Many researchers in the past have exploited the principle of impedance change to design novel biosensors in which the antibody-mediated binding of cells to electrode surfaces or the release of ions or other osmolytes by cells in suspension is used as the signal transduction mechanism for cell detection (Cheng et al., 2007; Suehiro et al., 2006; Venkatanarayanan et al., 2013; Yang, L., 2008; Yang et al., 2004). The sensitivity of signal achieved in these systems largely depends on the type of buffer used, the design layout of the biosensing electrodes, conditions of the applied AC electric field and the appropriate use of signal amplification probes (if any). As a consequence, while several studies exist on impedance-based detection and bacterial cell monitoring, very few of them report limits of detection below 10^4 CFU/mL (Varshney and Li, 2008; Yang et al., 2004; Zhu et al., 2010). We believe that the signal saturation at low concentrations is mainly due to the poor choice of operating parameters which greatly affect the quality of the final signal outcome.

In this paper, we investigate different experimental parameters to demonstrate how model S. typhi cells can be very sensitively and specifically detected in buffer using the impedance spectroscopy technique. For this purpose, micron-gap interdigitated electrodes (IDEs) were used to generate high electric field gradients near the electrode edges to improve the signal collection efficiency (Van Gerwen et al., 1998) (Fig. S1). This helped in enhanced monitoring of small changes taking place near the cell's microenvironment. To achieve the stringent limits of biorecognition specificity and sensitivity required for clinical applications, the bacterial cells were tagged with antibody-conjugated Au NPs and the changes in impedance response were measured before and after particle binding (Fig. 1). The signal from the bound Au NPs was used to quantify the number of cells present in 10 μL of sample within 5 min of its loading into the sensor. Using this approach, cell concentrations as low as 10 CFU/mL could be picked up easily, however, the specific detection threshold of our device (tested against E.coli. bacteria) was seen to lie at 100 CFU/mL.

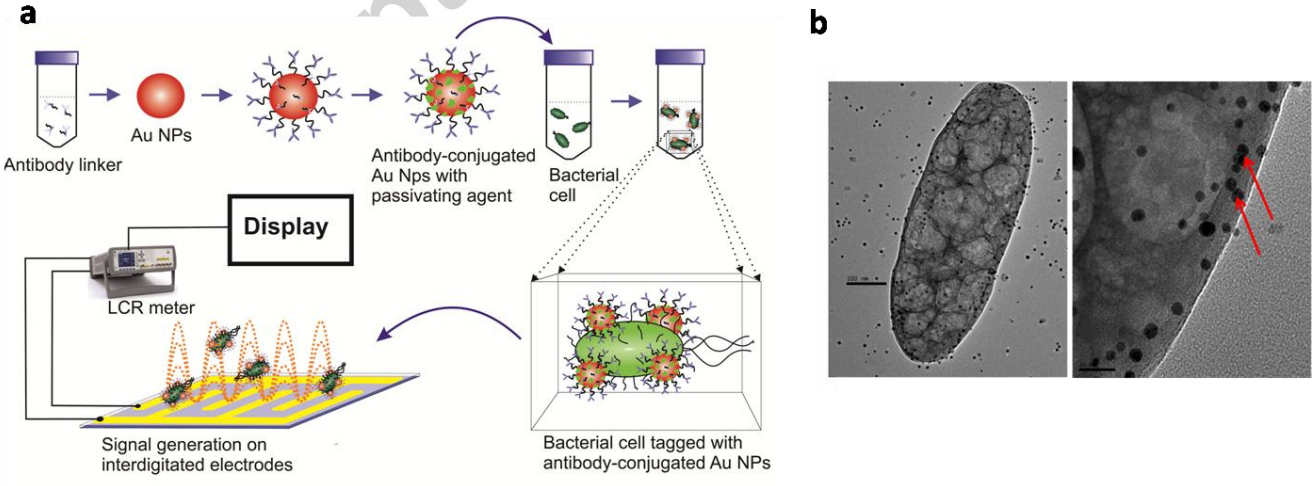

Fig. 1. (a) Schematic of the sample preparation and impedance sensing protocol. (b) TEM micrographs showing S. typhi cells tagged by Au-NPs (NP marked by arrows).

2. Experimental Section

2.1. Materials

Chloroauric acid ($HAuCl_4.3H_2O$), sodium citrate, phosphate buffer saline (PBS) and 4-(2-hydroxyethyl)-1-piperazineethanesulfonic acid (HEPES) were purchased from Sigma-Aldrich (India). Tannic acid, ammonium persulfate, sodium phosphate salts, sodium periodate, tween 20 and purpald were procured from Fisher Scientific (India). PEG_6-hydrazide aromatic dialkanethiol linker [M.W. 708.19 Da] was purchased from SensoPath Technologies (USA). Bovine serum albumin (BSA), carboxy-thiolpolyethyleneglycol (PEG-thiol) [M.W. 634.77 Da] and polyclonal antibody against Salmonella spp. in Rabbit antisera were sourced from Calbiochem (India), Thermo Scientific (India) and BD Biosciences (India), respectively. Luria bertani broth and Luria bertani agar were procured from Himedia Laboratories Pvt. Ltd. (India). Polydimethylsiloxane (PDMS) elastomer, silicone grease and 30 kDa MWCO centrifuge filters were purchased from Dow Corning (USA), Metroark (India) and Millipore India Pvt. Ltd., respectively. Ultrapure deionized (DI) Millipore water (resistivity ~18 MOhm.cm) was used for preparing all the buffers. All reagents were used as received.

2.2. Methods

2.2.1. Bacterial cell culture and sample preparation. A scoop of S. typhi bacteria was transferred from agar plates (Nims 90 ×15 mm) to 3 mL of Luria-Bertani broth at 37°C and cultured for 12 to 14 h. The cells were then centrifuged twice at 5500 rpm for 10 min (REMI RM-12C BL). Each time the supernatant was replaced with 0.1% v/v tween 20 solution in pH 8.5 HEPES buffer (hereby referred to as HT buffer). This washing step allowed the removal of any ionic residues from the growth medium. The stock culture suspension with 10^9 CFU/mL concentration was serially diluted with HT buffer down to a concentration of 10 CFU/mL. The concentration of

cells before and after serial dilution was determined using two methods – (i) the surface plating technique in which 10 μL of the cell suspension was streaked on agar plates at 37 °C and the number of colonies formed were counted after 16 to 18 h, and (ii) the optical density (O.D.) approach in which the concentration of the cell suspensions was measured at 600 nm wavelength with a UV-visible spectrophotometer (Shimadzu UV-2600). The entire procedure was repeated for the growth and preparation of E.coli samples used as controls in our study.

2.2.2. Antibody conjugation to Au NPs. Citrate-capped Au NPs, ~ 16 nm in size, were synthesized using a standard protocol available in the literature (Slot and Geuze, 1985). Briefly, a mixture of two solutions, solution A containing 1% w/v $HAuCl_4$ in ultrapure DI water and solution B containing 1% w/v sodium citrate and 0.1% w/v tannic acid in ultrapure DI water was heated at 60 °C for 4 h. The appearance of wine red color indicated the formation of Au NPs. The suspension was removed from heat and immediately chilled in an ice-bath to quench the reaction. The prepared Au NPs were then covalently conjugated to anti-S. typhi antibodies following the protocol by Kumar et al. (Kumar et al., 2008). In brief, 215 μL of 1 mg/mL antibody solution was diluted with 79 μL of 100 mM phosphate buffer at pH 7.4. A 10 μL volume of 100 mM sodium periodate was added to the above solution to partially oxidate the hydroxyls present in the glycosylated Fc region of the antibodies. The mixture was incubated in the dark for 30 min at room temperature and then the reaction was quenched with 500 μL of 10 mM PBS at pH 7.4.

The success of the partial oxidation reaction was determined by mixing 20 μL of the above antibody solution with 60 μL of freshly prepared 0.1 g/mL purpald solution prepared in 1 M sodium hydroxide. The turning of the solution to purple color within a few minutes indicated the successful formation of aldehydes. The remaining antibody solution was mixed with 10 μL of

9.3 mM hydrazide linker solution in absolute ethanol (99% purity). The mixture was then incubated for 1 h at room temperature followed by 1 mL addition of 40 mM HEPES buffer at pH 8.5. This entire volume was filtered using a 30 kDa MWCO centrifuge filter at 12000 rpm for 15 min to remove the excess linker. The retained antibody-linker solution was resuspended in HEPES buffer to a final volume of 1 mL and refrigerated at 4 °C for future use.

The antibody-linker was added to the 3.65 nM Au NP suspension in 5× molar excess. The mixture was vortexed for 1 min and incubated for 45 min. The suspension was then centrifuged at 5500 rpm for 15 min and the slightly pink supernatant was discarded to remove any unconjugated antibodies. The fluid pellet was resuspended in HT buffer containing additional blocking agents such as BSA (final concentration equal to 0.1 or 1% w/v) or PEG-thiol (7.5 mM final concentration) to prevent non-specific interaction of the NPs with the cells and of the cells with the antibodies specific to any other cell. After incubating with either blocking agent for 45 min, the suspension was again centrifuged at 5500 rpm for 15 min to remove the unbound blocking agent and the antibody-conjugated Au NPs were finally suspended in HT buffer at a concentration of 3.65 nM. The suspension was found to be stable at 4 °C up to at least a month.

2.2.3. Particle characterization. The size and morphology of the citrate-stabilized Au NPs were determined using Transmission electron microscopy (TEM) (FEI Tecnai G2). Images of 90 particles were taken and analyzed using the free ImageJ software (version 7). The results indicated near spherical particles with an average size of 16 ± 4 nm (Fig. S2). The concentration of the Au NPs was determined by UV-visible spectroscopy and found to be 3.65 nM upon synthesis (Slot and Geuze, 1985; Haiss et al. 2007). UV-visible spectroscopy was also used to confirm the antibody functionalization and stability of the Au NPs where a small red-shift of 3

nm in the absorbance spectra after conjugation, due to local surface plasmon resonance effects, suggested the presence of antibodies on the surface of the NPs (Fig. S3).

The optimization of molar ratio of antibody to Au NPs to achieve maximum coverage was performed using the gel electrophoresis method. The circular gel electrophoresis (CGE) setup was fabricated in our lab and consisted of a negatively charged graphite electrode at the center and a positively charged circular graphite electrode at the outer edge (Fig. S4a). A 1% w/v agarose gel was prepared in DI water by bringing the mixture to a boil at 130 ^{o}C and then pouring it in the circular petridish. A comb was inserted in the gel to make ~ 20 μL size wells. Once the gel was set, the comb was pulled out and the NP samples were loaded into the wells. A voltage of 20 V was applied which caused the particles to move radially outwards under the electric field in proportion to the amounts of antibodies conjugated to their surface (Fig. S4b). The minimum concentration at which the relative distance moved by the particles became insignificant with respect to the next higher concentration was termed as the optimal concentration for maximum coverage.

2.2.4. Au NP-tagging of bacterial cells. Different concentrations of 1 mL S. typhi and E.coli cell suspensions were incubated with 100 μL of 3.65 nM antibody-conjugated Au NPs (final NP concentration of 0.33 nM). The particles were kept incubated with cells in molar excess for 2 h with gentle shaking by hand every 15 min to ensure maximum binding. The suspensions were then washed twice at 5500 rpm for 15 min with HT buffer to remove any unconjugated NPs. The extent of NP-tagging of the bacterial cells was confirmed by TEM.

2.2.5. Experimental setup and data acquisition. The experimental setup consisted of a high precision LCR meter (20 Hz – 2 MHz, E4908A, Agilent) interfaced with interdigitated platinum microelectrodes on glass substrates. Each chip consisted of a total of 50 symmetrical finger

electrodes which were 100 µm wide and 100 µm spaced. The microelectrodes were encapsulated in a 1.5 mm thick PDMS slab punched with a 20 µL capacity hole to hold the samples. The PDMS chamber was sealed to the glass surrounding the electrodes by heating at 75 °C for 5 min. The time and temperature of heating were optimized to minimize sample leakage. 10 µL of sample was then inserted into the PDMS chamber and the top was sealed by a cover slip via vacuum grease to avoid evaporation. An AC field of 10 mV and 0.1 MHz frequency was applied and the data were collected every 2.5 min for 1 h. Each experiment was repeated at least thrice and the results were reported as the impedance change with respect to the HT buffer to account for any drift in signals due to unavoidable leakages or possible polymer swelling effects. Only the results for cell-particle biocomposites in the final assay were reported as the difference in impedance with respect to the cells alone. The electrodes were reused after extensive washing with acetone and DI water.

3. Results and Discussion

A number of different parameters affecting the system's impedance response were systematically investigated including applied frequency, incubation time, cell concentration, extent of antibody conjugation to NPs, type of blocking agent and the presence of a non-specific cell in the analyte such as E.coli.. Each of these parameters was individually optimized as discussed below to develop a robust biosensing device capable of detecting low concentrations of bacteria in the limit of clinical-relevance.

3.1. Selection of the electric field parameters for impedance immunosensor.

The first set of experiments was performed by taking impedance readings of buffer alone using a frequency sweep from 1 kHz to 1 MHz (Fig. S5). The signal dropped significantly upon increasing the

frequency up to 0.1 MHz and then eventually stabilized. This was expected because the ionic double layer capacitance developed at the electrode-liquid interface decreases inversely proportional to frequency until a critical relaxation frequency is reached (Gupta et al., 2012). Beyond this limit, the ionic capacitance can no longer exist and the medium resistance due to conduction of free ions takes over and starts to dominate the total impedance response of the system (Fig. S5). To ensure that the cell suspension conductivity was measured at the highest signal to noise ratio without the capacitance buildup at the electrodes masking the total signal, we decided to operate our device in the latter regime fixing the frequency at 0.1 MHz for all subsequent experiments.

The next set of impedance measurements were carried out to see the effect of incubation time in the sensor. Readings were taken with both plain and antibody-conjugated Au NPs, and their corresponding change in signal with respect to buffer was plotted at 0.1 MHz (Fig. 2a). In both cases, the signal was observed to be largely time-independent and higher than the buffer alone, however, the magnitude of impedance was much higher for the unconjugated NP suspensions. The greater change in impedance compared to buffer probably results from the fact that metallic Au NPs being perfect conductors create local obstructions in the ionic current flow by bending electric field lines perpendicularly inward into their surface and lowering the effective field present for current flow (Fig. S6a). This bending effect is partially offset by the presence of dielectric antibodies on the NP surface causing a smaller impedance change than pure metallic particles. On the other hand, time has little effect on the impedance spectra since the NPs remain homogeneously suspended in buffer due to Brownian motion.

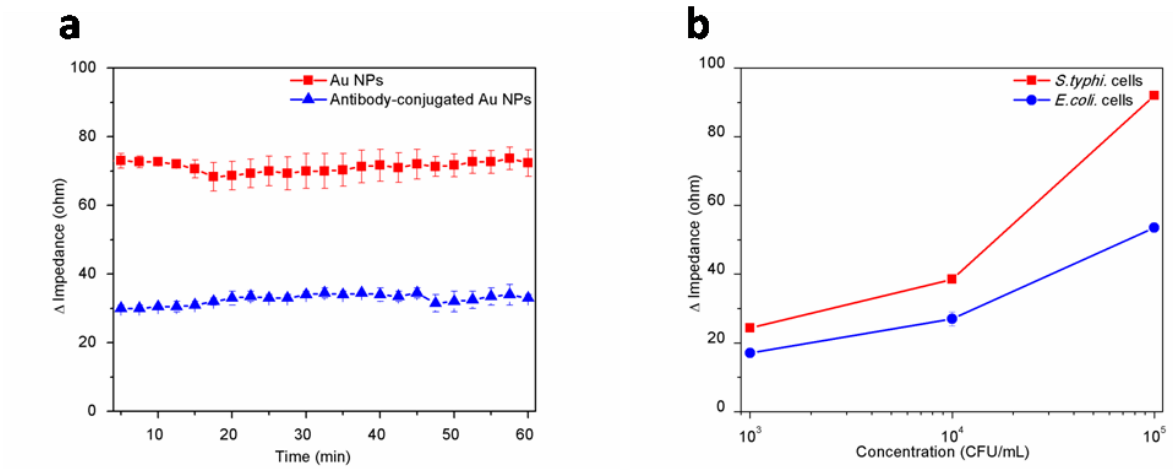

Fig. 2. (a) Time-lapsed impedance response of 3.65 nM Au NPs before and after antibody-conjugation (b) Concentration-dependent impedance measurements of S. typhi and E.coli. cells. Data collected 5 min after sample loading. AC field conditions used were10 mV and 0.1 MHz. The error bars where not seen are smaller than the data points.

When the impedance experiments were similarly repeated with 10^5 CFU/mL of S. typhi and E.coli. cell suspensions, they too showed that the signal was time-independent for at least up to an hour (Fig. S7). This led us to fix the sensor operating time at 5 min for all subsequent data collection. It may be noted that the time period for this duration may change if the cells are non-viable since the dead cells tend to settle down faster due to gravitational effects. Impedance increased as a function of cell concentration (Fig. 2b) suggesting that the cells also impede current flow by behaving as conductors similar to the case of Au NPs. This is not surprising considering that the cytoplasmic cell interior has high ionic content having conductivity as large as 1 S/m, almost four times higher than the background buffer conductivity used in our experiments (Wang et al., 2012; Yang, L., 2008).

Some earlier studies have reported an opposite trend for cell concentration-dependent impedance variation, different from what we observe, which occurs if the suspension gradually becomes more conductive due to the ions released by the cells into the media. We did not, however, see this happen in our case due to the specific way our samples were prepared. The

differences in impedance values between the two cell types is likely caused by the intrinsic variations in their morphology which in turn may be exploited for sensitive and label-free biosensing.

3.2. Effectiveness of the dilution technique. All the bacterial samples used in the above experiments were prepared using the serial dilution method. Since this method may introduce unforeseen experimental errors in our results, we decided to first check the effectiveness of the dilution approach with the plating method accepted widely as the gold standard in the pharmaceutical industry. To this end, different dilutions of S. typhi and E.coli cells were prepared in the range of 10^2 to 10^7 CFU/mL starting from a 10^9 CFU/mL stock suspension. Each sample was split into two parts, one of which was plated on the agar plates and the other was used for measuring its optical density (O.D.). The results showed good correlation between the dilution order and the cell plating concentration confirming the effectiveness of the serial dilution approach used in our studies (Fig. 3).

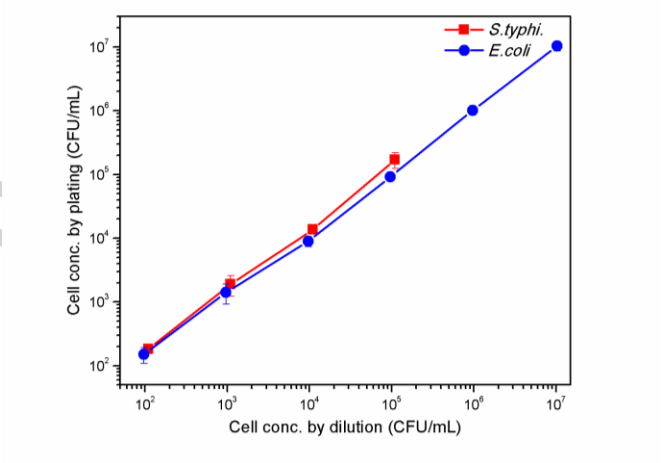

Fig. 3. Benchmarking of the serial dilution technique against the industrially-accepted surface plating method showed good cross-correlation. The error bars where not seen are smaller than the data points.

3.3. Optimization of antibody conjugation. The facile directional self-assembly of the antibodies on the NPs was carried out via a heterobifunctional linker attached to the Fc region of the antibodies via a hydrazine bond on one end and to the gold surface through thiol appendages on the other, leaving the Fab portion available for antigen targeting. To determine the minimum number of antibodies required to optimally cover the entire particle surface area, antibodies were conjugated with Au NPs in molar ratios varying from 1:1 to 10:1. This range of ratios was chosen based on the theoretical estimates considering the NP and antibody dimensions (see SI). The particles were then washed and subjected to a constant radial DC electric field using CGE. The particles moved from the negative to positive electrode in all the cases, however, the extent of distance travelled by them decreased linearly with surface coverage until the signal reached saturation around 5:1 molar ratio (Fig. 4a and S4b).

The electrophoretic velocity of the particles v in an applied electric field E is related to their mobility μ as $v = \mu E$, where μ is defined as $2\varepsilon\zeta f(\kappa R)/3\eta$ from the Henry equation (Medrano et al., 2009; Ohshima, H., 2001). Here, ε is the permittivity and η the viscosity of the gel matrix, ζ is zeta potential of the NP, κ is the inverse Debye length, R is the particle radius and $f(\kappa R)$ is a factor that lies between 1 and 1.5. Since, the velocity varied linearly with zeta potential in Fig. 4a and all other parameters remain constant in the Henry eqn, it can be deduced that the zeta potential of the antibody-conjugated NPs reduced by approx. 4.5 times before reaching saturation. The zeta potential of the unconjugated NPs was measured to be - 38.5 mV due to the presence of abundant citrate capping groups on the NPs (data not shown) which implied that the zeta potential of the 5:1 antibody-conjugated NPs was – 8.5 mV. We further confirmed our surface saturation results by taking impedance measurements of antibody-conjugated NPs at three different relative concentrations (Fig. 4b). The impedance response also saturated at 5:1

molar ratio verifying this to be the optimal concentration for antibody binding to be used in all the subsequent experiments. The number of antibodies bound to the Au NPs seems reasonable from coarse theoretical geometrical calculations and match the values given in literature (Kumar et al., 2008).

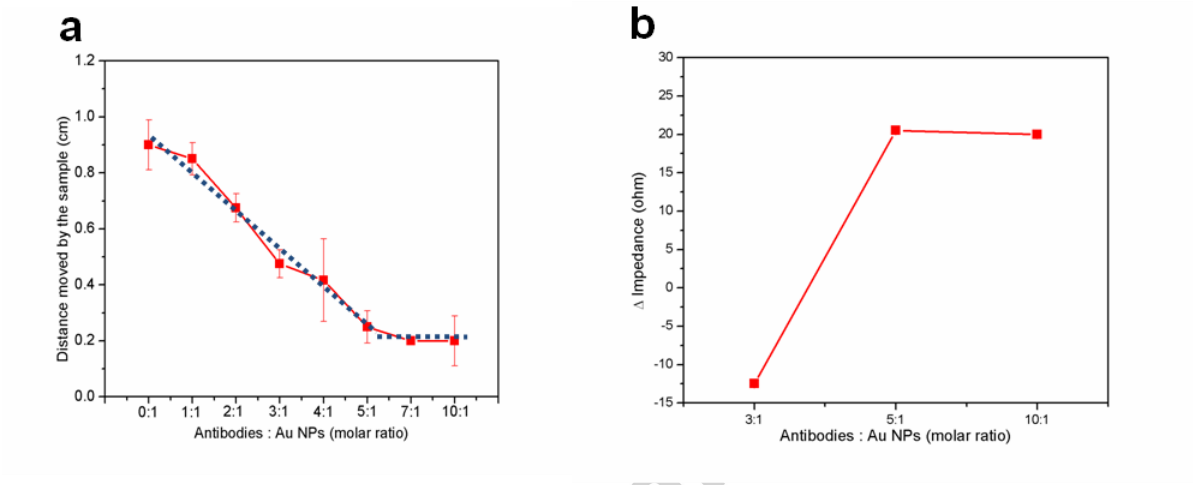

Fig. 4. (a) Distance moved by the antibody-conjugated Au NPs in the gel electrophoresis setup. (b) Saturation in impedance response upon increasing the antibody concentration with respect to the Au NPs. The data is measured 5 min after loading the sample on the chip. The error bars where not seen are smaller than the data points.

3.4. Immunosensing using biofunctionalized Au NPs as detection probes. A diagnostic device that discriminates infection due to one type of pathogenic bacteria from another is extremely useful in a clinical setting as it helps the physician decide the appropriate line of therapeutic management depending on the causative agent. Although broad-spectrum antibiotics are able to contain most bacterial infections, their usage needs to be carefully monitored against the alarming increase in drug resistance cases. Administering drugs to a patient who potentially harbors drug-resistant bacteria could not only adverse prognosis but also aggravate their medical condition further. With these considerations in mind, we tested the sensitivity and specificity of our biosensor towards discriminating small quantities of S. typhi bacteria against large

concentrations of E.coli. used as negative control. The limit of detection (LOD) was defined as the lowest concentration of S. typhi cells detected having signal higher than the response from 10^7 CFU/mL E.coli. cells. This upper limit of 10^7 CFU/mL considered "background noise" was chosen presuming that the bacterial concentrations do not generally exceed beyond 10^7 CFU/mL in most healthcare applications.

S. typhi and E.coli. cells were both tagged with anti-S. typhi antibody-conjugated Au NPs and their impedance spectra were independently measured as a function of cell concentration. The experiments were performed in the presence of two common blocking agents namely BSA and PEG to also study the effect of surface passivation which is a necessary step in evaluating any biosensor performance and to ensure specificity of signal. The results were reported as the difference in impedance from the cell-particle bioconjugates and the cells taken alone at the same concentration. In other words, the final signal reported was a contribution only from the bound Au NPs. This was done to find the cut-off value for non-specific binding of the NPs to the non-targeting cells, in this case E.coli.

The operating conditions for the blocking agents were optimized before proceeding to the sensitivity determination of the bioassays. BSA minimizes non-specific interaction by readily adsorbing at the solid-liquid interface typically within a few minutes (Boulos et al., 2013; Brewer et al., 2005). When a high 1% w/v concentration of BSA was used, the impedance signal of the chip was completely flooded making it impossible to distinguish between the results from cells alone or the cells tagged with Au NPs (Fig. S8a). A 10 times diluted BSA concentration, on the other hand, did not pose this problem (Fig. S8b). Similarly, the conditions for the PEG-thiol blocking agent, which attached to the NPs via covalent thiol linkages, were optimized separately (Fig. S9).

The bioassays performed with 0.1% w/v BSA gave an LOD of 10^5 CFU/mL and the lowest distinguishable limit between S. typhi and E.coli. samples was 10^4 CFU/mL (Fig. 5a). Both the LOD and the minimum discernable limit improved by an order of magnitude to 10^4 and 10^3 CFU/mL, respectively, upon changing the blocking reagent from BSA to PEG (Fig. 5b). Another important noticeable difference in the two blocking schemes was that the overall impedance response for S. typhi samples remained more or less constant, whereas, it reduced drastically in the case of E.coli. cells when using PEG. This highlights the fact that the NP binding to E.coli. cells was actually non-specific in nature and could be reduced by choosing an appropriate blocking reagent. To further push the sensitivity limits of detection in order to make the immunosensor more applicable for a clinical setting, we incorporated a small additional step during the sample handling procedure. During the final centrifugal washing step in the cell-particle conjugation protocol, we preconcentrated the sample 100 times (from 1 mL to 10 μL) and reproducibly achieve an LOD as low as 10^2 CFU/mL with a differential limit of just 10 CFU/mL (Fig. 5c). These results suggest that the detection of infectious diseases such as typhoid in the initial periods of illness can be made possible with minimal intervention given that the right set of parameters are chosen for operating the biosensor. One of course needs to pay careful attention to the signal contributions brought about by the blood cells and the proteins in the complex media and this has currently formed the basis of our further studies. Our results, so far, are in accordance with some of the best impedance-based bacterial immunosensors reported in the literature (Fung and Wong, 2001; Oh et al., 2004; Radke and Alocilja, 2005; Salam and Tothill, 2009; Yang and Bashir, 2007; Yang et al., 2009; Yang, L., 2008).

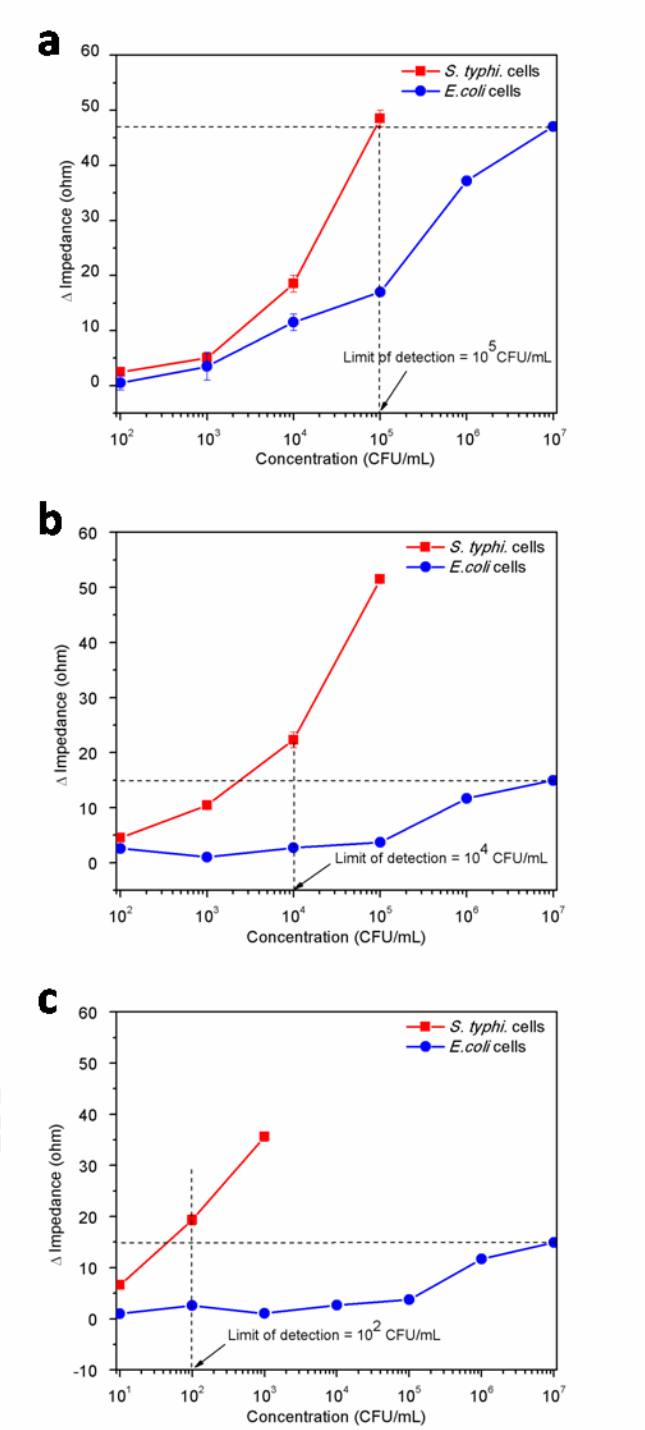

Fig. 5. Specific bioassay response obtained as a function of cell concentration using two different blocking agents and varying preconcentration conditions: (a) with 0.1% w/v BSA, (b) with 7.5 mM PEG-thiol and (c) with 7.5 mM PEG-thiol after 100 times centrifugal pre-enrichment. The error bars where not seen are smaller than the data points.

4. Conclusions

We have demonstrated that the impedance spectroscopy technique employing reusable surface patterned electrodes and functionalized NPs is a versatile approach for simple, rapid, and sensitive detection of typhoid-causing S. typhi bacteria. The specific cell-labeling with Au NP probes and the proper choice of frequency and blocking agent allowed us to achieve a reasonably low detection limit of 100 CFU/mL with very little resources. In future, our approach could potentially be used for high-throughput screening of clinical as well as parenteral pharmaceutical products.

5. Acknowledgements

We thank Shouri Chatterjee (EE-IITD) for providing the LCR meter, Vinay Gupta (Physics-DU) for fabricating the microelectrodes, Vivekanandan Perumal and Mohita Upadhyay (KSBS-IITD) for teaching the method of bacterial cell inoculation and providing the bacterial strains, and Mikhil Raj (ME-IITD) for fabricating the CGE setup. NP thanks IITD for providing her the fellowship to carry out this research.

6. References

1. Ahmed, O.B., Asghar, A.H., El-Rahim, I.H.A., Hegazy A.I., 2014. J. Bacteriol. Parasitol. 5, 5–7.
2. Boulos, S.P., Davis, T.A., Yang, J.A., Lohse, S.E., Alkilany, A.M., Holland, L.A., Murphy, C.J., 2013. Langmuir 29, 14984−14996.
3. Brewer, S.H., Glomm, W.R., Johnson, M.C., Knag, M.K., Franzen, S., 2005. Langmuir 21, 9303–9307.
4. Cheng, X., Liu, Y., Irimia, D., Demirci, U., Yang, L., Zamir, L., Rodriguez, W. R., Toner, M., Bashir, R., 2007. Lab Chip 7, 746–755.
5. Fung, Y. S.; Wong, Y. Y., 2001. Anal. Chem. 73, 5302-5309.
6. Garibyan, L., Avashia, N., 2013. J. Invest. Dermatol. 133, 1-4.
7. Gervais, L., Rooij, N. De, Delamarche, E., 2011. Adv. Mater. 23, H151–H176.
8. Gupta, S., Kilpatrick, P.K., Melvin, E., Velev, O.D., 2012. Lab Chip 12, 4279–86.
9. Haiss, W., Thanh, N.T.K., Aveyard, J., Fernig, D.G., 2007. Anal. Chem. 79, 4215–21.

10. Khandurina, J., Mcknight, T.E., Jacobson, S.C., Waters, L.C., Foote, R.S., Ramsey, J.M., 2000. Anal. Chem. 72, 2995–3000.
11. Ko, S., Grant, S., 2006. Biosens. Bioelectron. 21, 1283–90.
12. Kumar, S., Aaron, J., Sokolov, K., 2008. Nat. Protoc. 3, 314–20.
13. Medrano, M., Perez, A.T., Lobry, L., Peters, F., Medrano, M., Perez, A.T., Lobry, L., Peters, F., 2009. Langmuir 25, 12034-12039.
14. Melvin, E.M., Moore, B.R., Gilchrist, K.H., Grego, S., Velev, O.D., 2011. Biomicrofluidics 5, 34113–3411317.
15. Oh, B.K., Kim, Y.K., Park, K.W., Lee, W.H., Choi, J.W., 2004. Biosens. Bioelectron. 19(11), 1497-1503.
16. Ohshima, H., 2001. J. Colloid Interface Sci. 239, 587–590.
17. Radke, S.M., Alocilja, E.C., 2005. Biosens. Bioelectron. 20, 1662–1667.
18. Salam, F., Tothill, I.E., 2009. Biosens. Bioelectron. 24(8), 2630-2636.
19. Sanders, G.H.W., Manz, A., 2000. Anal. Chem. 19, 364–378.
20. Slot, J.W., Geuze H.J., 1985. Eur. J. Cell Biol. 38, 87-93.
21. Suehiro, J., Ohtsubo, A., Hatano, T., Hara, M., 2006. Sensors Actuators B 119, 319–326.
22. Tsai, H., Tsai, Y., Yagur-kroll, S., Palevsky, N., Belkin, S., Cheng, J., 2015. Lab Chip 15, 1472–1480.
23. Van Gerwen, P., Laureyn, W., Laureys, W., Huyberechts, G., Op De Beeck, M., Baert, K., Suls, J., Sansen, W., Jacobs, P., Hermans, L., Mertens, R., 1998. Sensors Actuators B Chem. 49, 73–80.
24. Varshney, M., Li, Y., 2008. Talanta 74, 518–25.
25. Venkatanarayanan, A., Keyes, T.E., Forster, R.J., 2013. Anal. Chem. 85, 2216-22.
26. Wain, J., Diep, T.O.S., Ho, V.O.A.N.H., Walsh, A.M., Thi, N., Hoa, T., Parry, C.M., White, N.J., 1998. J. Clin. Microbial. 36, 1683–1687.
27. Wang, Y., Ye, Z., Ying, Y., 2012. Sensors 12, 3449–71.
28. Wen, C., Hu, J., Zhang, Z., Tian, Z., Ou, G., Liao, Y., Li, Y., Xie, M., Sun, Z., Pang, D., 2013. Anal. Chem. 85, 1223−1230
29. Yadav, V.G., Brigham, M.D., Ling, Y., Rivest, C., Demirci, U., Khademhosseini, A., 2006. Micro and Nanoengineering for High-Throughput Biomedical Applications, in: Shi, D. (Ed.), Nanoscience and Its Applications in Biomedicine. Springer-Verlag and Tsinghua University Press, pp. 314-46.
30. Yang, G., Huang J., Meng, W., Shen, M., Jiao, X., 2009. Anal. Chim. Acta 647, 159–166.
31. Yang, L., 2008. Talanta 74, 1621–1629.
32. Yang, L., Bashir, R., 2008. Biotechnol. Adv. 26, 135–50.
33. Yang, L., Li, Y., Erf, G.F., 2004. Anal. Chem. 76, 1107–13.
34. Yang, L., Li, Y., Griffis, C.L., Johnson, M.G., 2004. Biosens. Bioelectron. 19, 1139–47.
35. Ye, R., 2010. Talanta 56, 1-15.
36. Yeo, L.Y., Chang, H.-C., Chan, P.P.Y., Friend, J.R., 2011. Small 7, 12–48.
37. Yoon, J.-Y., Kim, B., 2012. Sensors 12, 10713–41.
38. Zhou, L., Darton, T., Waddington, C., Pollard, A.J., 2012. Molecular Diagnosis of Enteric Fever: Progress and Perspectives, in: Annous, B.A., Gurtler, J.B. (Eds.), Salmonella – Distribution, Adaptation, Control Measures and Molecular Technologies. InTech, pp. 429-52.

Highlights

1. We demonstrate the use of impedance spectroscopy, reusable patterned electrodes and surface-engineered Au NPs as a versatile approach for simple, rapid, and sensitive detection of typhoid-causing S. typhi bacteria in spiked buffer samples.

2. We emphasize on the critical choice of operating parameters such as electric field frequency, orientation of antibody binding on the Au NP probes, surface blocking agents etc. to achieve low detection limits of 100 CFU/mL in only 10 μL of sample within 5 min of loading the sample.

3. Our sensitivity limits match some of the best cited studies in the literature on this topic and potentially show great promise for high-throughput screening of clinical samples. The technique could be extended to characterizing cell and colloidal particle concentrations in unknown samples.